Volcanic synchronisation between the EPICA Dome C and Vostok ice cores (Antarctica) 0-145 kyr BP

Frédéric Parrenin (1, 2); Jean-Robert Petit (2); V. Masson-Delmotte (3); I. Basile (4); J. Jouzel (3);

V. Lipenkov (5); Sune Rasmussen (6); Jakob Schwander (7); Mirko Severi (8); Roberto Udisti (8);

Daniel Veres (2); Bo Vinther (6); Eric Wolff (9)

(1) Laboratoire Chrono-Environnement, Besançon, France.

(2) Laboratoire de Glaciologie et Géophysique de l'Environnement, Grenoble, France.

(3) Laboratoire des Sciences du Climat et de l'Environnement, Gif-sur-Yvette, France.

(4) Centre Européen de Recherche et d'Enseignement des Géosciences de l'Environnement, Aix-en-Provence, France.

(5) Arctic and Antarctic Research Institute, St Petersburg, Russia.

(6) Centre for Ice and Climate, Niels Bohr Institute, University of Copenhagen, Copenhagen, Denmark

(7) Physics Institute, University of Bern, Bern, Switzerland.

(8) Department of Chemistry, University of Florence, Florence, Italy.

(9) British Antarctic Survey, Natural Environment Research Council, Cambridge, UK

Abstract

This study aims at refining the synchronisation between the EPICA Dome C (EDC) and Vostok ice cores in the time interval 0-145 kyr BP by using the volcanic signatures. 111 common volcanic events were identified by using continuous electrical conductivity (ECM), di-electrical profiling (DEP) and sulfate measurements while trying to minimize the distortion of the glaciological chronologies. This is an update and a continuation of previous works performed over the 0-45 kyr interval which provided 56 tie points to the ice core chronologies [Udisti et al, 2004]. This synchronisation will serve for the establishment of the next synchronised Antarctic dating. A change of slope in the EDC-depth/Vostok-depth diagram is probably related to a change of accumulation regime as well as to a change of ice thickness upstream of the Vostok lake, but we did not invoke any significant temporal change of surface accumulation at EDC relative to Vostok. A significant phase difference is detected between the EDC and Vostok isotopic records during the 95 - 120 kyr

interval, but not during Termination II. Three possible candidates for the Toba volcanic super-eruption ~73 kyr ago are suggested in the Vostok and EDC volcanic records. However the ECM, DEP and sulfate fingerprints for these three events are not significantly larger than many others in the records.

1 Introduction

Ice cores drilled in polar areas are natural archives of past environmental and climatic conditions on the Earth. They can ~~depict~~ past atmospheric composition and climatic variability for time periods spanning up to several hundreds of millennia in Antarctica [Petit et al., 1999; EPICA community members, 2004; Jouzel et al., 2007] with time-resolution higher than annual for at least the last 60 kyr in some Greenland sites [Vinther et al., 2006; Svensson et al., 2008]. However, in order to interpret such records in a paleoclimatic context, there is the need to constrain the age duration of the former climatic events recorded in the ice matrix (eg., water isotopes, chemical proxies, dust) or in the gaseous species trapped within the ice.

Numerous strategies are currently applied ~~for~~ dating the ice matrix and the gas phase ~~along~~ ice cores: (i) wiggle matching of ice core records to insolation time series (i.e., orbital tuning) [e.g., Waelbroeck et al., 1995; Parrenin et al., 2004; Dreyfus et al., 2007; Kawamura et al., 2007], (ii) wiggle matching of ice core records to other dated paleo-archives such as ice, marine or terrestrial cores [e.g., Blunier et al., 2001; Waelbroeck et al., 2008], (iii) identification of dated horizons such as tephra layers, sulfate spikes or cosmoegenic radionuclides spikes [e.g., Castellano et al., 2005; Narcisi et al., 2006; Severi et al., 2007; Raisbeck et al., 2007], (iv) counting of annual layers [e.g., Svensson et al., 2008 and references therein] and (v) ice flow modeling [e.g., Parrenin et al., 2007a; Salamatin et al., 2009a], combined with firn densification modelling to estimate the ice-gas age difference (Δage) [Goujon et al., 2003; Salamatin et al., 2009b].

Despite these efforts, when comparing records from different sites, even on the same ice-sheet, age offsets always appear. The first step toward the construction of a common age model for ice-cores is the synchronisation between glaciostratigraphies, i.e. the relative matching of profiles obtained within the same drill site (over distances from a few meters to kilometers) and among different drilling sites.

The drilling of ice sheets and the recovery of continuous ice sections is indeed not a simple process. Due to technical or other site specific drilling constraints usually several ice cores were needed to recover the whole ice column down to the base of the glacier at many drilling sites. For the EPICA Dome C project, only two long ice cores were drilled (see Figure 1). The first one commenced

65 during the 1996/1997 season (EDC96) and reached ~790 m where the drilling system got stuck while the second one started during the 1999/2000 (EDC99, only around 10 m from EDC96 at surface, this distance varying in depth due to different hole inclinations) season and stopped near the bedrock, at ~3260 m depth. During the 1998/9 season at EDC a shallow hole named Firetracc was drilled 200 m SW of the deep drill site for sampling firn air, providing ~~also~~ an extra ice core to

70 a depth of 120 m. For Vostok, several cores ~~were~~ drilled since the initiation of the project in 1975 [see Vasiliev et al., 2007, for a review]. For the present study (Figure 2 and Figure 3), we used the isotope profile from VK-3G core (started in 1980 and reached 2083 m) which represents the first Antarctic climatic record covering the last glacial cycle [Lorius et al, 1985]. The record was supplemented for the upper part by the isotope record from VK-4G (started in 1983 and reached

75 2546 m depth). The continuous ECM record was performed on VK-5G (started in 1990 and reached 2503 m depth), and the record was complemented for the upper part by a couple of shallow cores from an electromechanical drill (VK-BH8 and VK-BH7 drilled during the 1995-1996 field season).

Some ice core synchronisation efforts have relied on matching of similar features in the isotope

80 profiles [Parrenin et al., 2007b]. This approach relies on the validity of two hypotheses: first, ~~the homogeneity of~~ the temperature ~~variability~~ for sites from a given ice sheet with presumably similar climatic conditions, e.g. over the East Antarctic Plateau [Watanabe et al., 2003], and second, the stability of the isotope temperature relationship. While climate models and meteorological observations and reanalyses confirm a coherency of inter-annual to decadal temperature fluctuations

85 on the East Antarctic plateau [Masson-Delmotte et al., 2011; Siddall et al., in press], the intermittency [Sime et al., 2009; Stenni et al., 2010; Laepple et al, 2011] of precipitation may induce site specific isotopic signals. Superimposed on this deposition variability, post depositional processes linked to wind erosion and depth propagation of surface height variability are known to induce noise in isotopic profiles, even at the local scale [Ekaykin et al., 2002]. Finally, uncertainties

90 ~~on~~ ice core isotopic synchronisation arise from different sampling resolutions. As an example of ice core synchronisation, the EDC3 age scale was transferred to the Vostok and Dome Fuji ice cores by synchronisation of the isotopic content of ice [Parrenin et al., 2007b]. It is therefore important to test whether the hypothesis of in-phase isotopic variations for climatic transitions or millennial-scale events is valid at regional to continental scale. Testing isotopic synchronisation therefore

95 requires using synchronisation methods independent of stable isotope records.

Volcanic signatures have this potential, and also offer sharp stratigraphic markers: the deposition typically spans 1-2 years, even for stratospheric events [Gao et al., 2006], which gives excellent accuracy to the synchronisation. Volcanic products (mainly ~~ash,~~ minerals, glass particles and SO_2,

rapidly oxidised to H_2SO_4) are emitted into the stratosphere and/or into the high troposphere during volcanic eruptions, deposited on the Earth's surface via wet and/or dry deposition and preserved in ice or sediment sequences as tephra layers and/or sulfate (and as a consequence acidity and conductivity) spikes [Gao et al., 2008]. Uncertainties in the matching of volcanic signatures arise from the fact that the distribution of volcanic aerosol particles (e.g. non-sea-salt-sulphate) and tephra can be affected by atmospheric transport and therefore may not be detected or detected with varying levels in Antarctic ice cores [Gao et al., 2008]. Ice cores from the same ice sheet are presumed to record similar volcanic signatures (both global and regional), even if some local events of very low intensity could be recorded only at local scale [Rasmussen et al., 2008]. The total volcanic deposition can greatly differ spatially depending on geographic location, atmospheric transport pathways and the ratio between wet and dry deposition contributions [Castellano et al., 2005; Wolff et al., 2005; Gao et al., 2006].

Moreover, the possibility to match ice-core records from different hemispheres by finding signatures of inter-hemispheric volcanic events (i.e. explosive tropical eruptions that could spread products into both hemispheres through the stratosphere) is complicated by the presence of signatures of local to regional events recorded in just one ice sheet. For example, the Toba super-eruption ~73 kyr ago is one of the most important of the last million years [e.g., Petraglia et al., 2007], with possible global and regional consequences such as climate cooling and deforestation in South Asia [Williams et al., 2009; Williams, in press], though the environmental impact of this eruption is debated [Robock et al., 2009]. Indeed, some of the environmental changes occurring after the Toba event may have been caused by the strong concurrent millennial-scale climate variability, the Toba super-eruption reportedly being coincident with the end of Greenland Interstadial (GI) 20 [Zielinski et al., 1996]. Chemical information from this large eruptive event should be recorded in both ice sheets. A possible candidate (a six years long sulfate spike exceptional in amplitude) has been proposed in the GISP2 ice core from Greenland [Zielinski et al., 1996] but none has so far been identified in Antarctic ice cores.

In this paper, we describe the stratigraphic correlation between the EPICA Dome C ice cores (EDC96 and EDC99) and the Vostok ice cores (BH7, 3G, 5G) records by using volcanic markers during the period 0-145 kyr BP. Previous studies compared Vostok and EDC96 Electrical Conductivity Measurements (ECM) profiles for the last 10 kyr [Wolff et al., 1999], and sulphate and ECM volcanic signatures in the EDC96 ice core back to 45 kyr BP [Udisti et al., 2000; Udisti et al., 2004]. Here we extend the comparison over the last 145 kyr, and synchronize the ice core depth scales independently from any dating model. We discuss possible leads/lags of the EDC isotopic record relative to the Vostok one, analyse the Vostok-depth / EDC-depth isochronal diagram

resulting from the volcanic synchronisation, and finally analyse the possible fingerprint of the Toba super-eruption in the Vostok and EDC ice cores.

135

2 Methods

2.1 The data

2.1.1 Depth measurements

The depth of an ice core is either measured from the drilling cable length or from the logging of the
140   ice cores, the later being more widely used. In case of broken ice cores, the logging depth uncertainty is increased. This is particularly problematic in the depth zone corresponding to the transition between air bubbles and clathrates, where the ice is particularly brittle due to post drilling pressure relaxation ("brittle zone"). This brittle zone ~~concerns~~ the depth interval 600 m – 1200 m at EDC and 300 m – 720 m at Vostok. For the Vostok ice core, the use of a thermal drill ~~dampens~~ the
145   ice core quality as a result of added thermal stress and it extends the depth of fractured ice cores down to ~850 m.

It is absolutely essential that all analyses made on an ice core are put on the same reference depth scale. Only the logging depth can provide such a scale, because drilling depth is not consistent from run to run due to errors from the encoder wheel and varying dynamic tension in the drill cable. To
150   put the records directly on an age scale is also not feasible, because chronologies are not absolute and will be improved in the course of time. A drawback of the logging depth is its offset to the true depth, which is used in glaciological models. This offset is due to the following reasons: (1) the hole is generally inclined and the core therefore longer than the vertical distance to the surface. (2) The core expands by elastic and plastic relaxation before logging (3) The temperature of the core when
155   logged is different from the in situ temperature. (4) The logging gauge is often calibrated at +20°C but used at negative temperatures. (5) Errors from marking and fitting the cores between runs and fitting broken cores (especially in the brittle zone). Offsets (1) to (4) can sum up to several meters for a deep drilling and could mostly be corrected for, but to our knowledge it has never been applied.

160   #### 2.1.2 ECM Data

The Vostok ECM data were acquired during several successive field seasons (from 1992 to 1998) ~~according to the advance of the drilling operations~~. The ECM system developed at Laboratoire de Glaciologie et Géophysique de l'Environnement (LGGE) was set up in the glaciological laboratory

building nearby the ice core storage and facilities on the site. After one overnight preheating at -15°C in a forced ventilated and insulated buffer, the full ice sections (1 m long, 10 cm diameter) were set on a tray on the bench and a first 1 cm slice was cut by using a horizontal saw. ~~A 1500 volts high tension was applied between two electrodes~~ (1mm^2 section in contact with ice) separated by 20 mm distance. The electrodes were moved over the fresh ice surface at a speed of 2 m/mn and the ECM signal was recorded by both digital and paper recorder systems. ~~As~~ tests ~~for~~ stability of the measurement chain and signal consistency between the different seasons, we used a 100 Mohm resistor (daily test) and repeated ECM measurement on selected ice core that were kept stored at -50°C (each season). The firn part of the upper VK-5G core was percolated by the water produced by the thermal drill, disturbing the ECM signal, which cannot be used. We therefore relied instead on the ECM record from two adjacent (4 m apart) deep electromechanically drilled cores (VK-BH8 down to 130 m and VK-BH7 down to 250 m respectively, drilled 400 m away from VK-5G). The composite ECM signal is from VK-BH8 from 6 m down to 130 m depth, from VK-BH7 from 130 m to 230 m, then from VK-5G below 230 m depth. Using the common volcanic events, depths from VK-BH8 and VK-BH7 were transferred to the VK-5G depth (logging depth), the latter taken as reference. Data reduction was done and aberrant events corresponding to ice core breaks were removed. The data were then re-sampled every centimetre.

At Dome C, a new system, developed at the University of Bern, was used. A flat surface was prepared along the 2.2 m length of a core using a horizontal band-saw and a milling device. The electrodes assembly consisted of seven electrodes at a spacing of 8 mm across the core. The electrodes were made of a carbon-doped silicon rubber. They were lowered onto the surface of the core, and 350 V was applied across each adjacent pair of electrodes in turn. The current between them was sampled at regular intervals after a settling time, and averaged. The electrodes were lifted and moved 1mm along the core before the sequence was repeated. This procedure yielded six sets of data at 1mm resolution. The data presented here are given as conductances averaged to 10 mm and corrected to -15°C. Documented major core breaks and ends have been removed from the ECM record. The Firetracc core was used for the top 100 m because measurements were not possible on the EDC96 and EDC99 ice cores due to logistic constraints.

2.1.3 DEP data

DEP data were obtained every 2 cm along the entire length of both the EDC96 and EDC99 cores. From the measured properties, a 100 kHz conductivity was derived at each depth step [Wolff et al., 1999]. Whereas ECM is believed to respond only to acidity, DEP conductivity responds to a wider range of impurities. However, under the conditions at Dome C, the signal is also almost always dominated by the acidity of the ice [Wolff, 2000].

2.1.4 Sulfate data

EDC96 sulphate analysis was performed in the field by Fast Ion Chromatography (FIC), obtained by coupling an ion-chromatographic (IC) system with a continuous flow analysis apparatus (Udisti et al., 2000). The system allowed 1 measurement per minute. Since the melting rate was kept constant at 4 cm/min, a resolution of 4 cm (ice equivalent) was obtained. During the EDC99 processing, two IC systems worked in a parallel way (30 s shifted) and the resolution was increased to 2 cm.
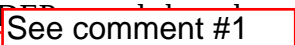
2.1.5 Stable isotope data

Both the deuterium (δD) and the oxygen 18 ($\delta^{18}O$) contents of the ice are commonly used to get information on past temperature changes in polar regions. Hereafter, we will use the δD profiles which were obtained at Laboratoire des Sciences du Climat et de l'Environnement (LSCE) both for the Vostok [Jouzel et al., 1987] and EDC cores [Jouzel et al., 2001, 2007 ; EPICA Community Members, 2004]. The measurements were conducted on samples extracted from a band along the ice cores. The same uranium reduction technique was used for all these measurements performed on home built mass spectrometers [Hagemann et al., 1978] with modifications being limited to the automatic injection device [Vaughn et al., 1998]. All along the measurement period, the same protocol - consisting of four injections for a given water sample with at least two independent measurements for each - has been followed allowing to reach a precision of $\pm$ 0.5 ‰ (1 s).

As fully described in Lorius et al. [1985] and Jouzel et al. [2007], the published Vostok δD record was obtained from the VK-3G 2083 m deep ice core below 138 m with a complementary dataset obtained on the adjacent VK-4G 279 m core. The sampling was conducted at low resolution with for example 1.5 to 2 m samples below 1400 m and a total ice recovery of 85% and some missing samples (sampling was particularly difficult in the 300 to 800 m range with missing samples on depth intervals of up to 8 m). Additional measurements have been more recently obtained on VK-4G and VK-5G [Petit et al., 1999 and unpublished data]. The EDC δD published profile was obtained with a higher 55 cm depth resolution on a continuous basis in combining measurements performed on EDC96 down to 788 m and on EDC99 below [Jouzel et al., 2007].

2.2 Synchronisation method

2.2.1 EDC96-EDC99 volcanic synchronisation

The [See comment #1] used to synchronize the EDC96 and EDC99 ice cores down to 790 m. 104 prominent pairs of spikes corresponding to volcanic events have been used to determine common age horizons (see Table 1 and Figure 4A).

230   The depth difference (see Figure 4B) ranges from ~0.05 m to ~0.75 m, EDC96 recording similar
       events at slightly deeper depths compared to EDC99. The depth difference remains largely confined
       between 0.1 and 0.3 m down to 600 m. The small oscillations in this depth interval are probably due
       to spatial irregularities of snow deposition/re-deposition [sastrugi, Ekaykin et al., 2002; Barnes et
       al., 2006]; the logging uncertainty could indeed only contribute a systematic error of order <1 mm
235   per 2.2 m. Between 600 and 790 m, the depth difference increases to ~0.7 m, probably due to
       logging differences between the two cores. Indeed, the 600 m depth corresponds to the start of the
       brittle zone at EDC.

       We use this EDC96/EDC99 synchronisation to anchor the EDC96 records on EDC99 depths. We
       assume that 1) the offset is 0.18 m at surface (this value corresponds to the shallower data point in
240   Table 1 and Figure 4); 2) the offset varies linearly between the volcanic tie points.

2.2.2   Vostok BH7-5G volcanic synchronisation

       The ECM records have been used to synchronize the BH7 and 5G ice cores in the depth interval
       where the records overlap, i.e. between 200 and 240 m. 6 pairs of spikes corresponding to volcanic
       events have been recognized in this interval and considered to represent common age horizons (see
245   Table 2 and Figure 5).

       The depth difference ranges between 3.25 and 3.43 m, 5G being deeper than BH7 for the same
       horizon. This shift is significantly larger than the 2.56 m shift determined at 104.68 m (depth in 5G)
       with the help of a tephra horizon (see Figure 3). We do not know at this stage if this increased offset
       is due to logging uncertainties or to a varying accumulation pattern.

250   We used this synchronisation to transfer the BH7 records on 5G depths. We assumed that 1) the
       offset is 0 at surface; 2) the offset varies linearly between the volcanic tie points (including the
       tephra horizon at 104.68 m 5G depth).

2.2.3   Vostok 3G-5G isotopic synchronisation during termination II

       On Figure 6 is plotted the ice isotopic composition for the Vostok ice cores 3G and 5G during
255   termination II. The 5G data are confined between 1800 and 1900 m depth. One can observe that a
       depth shift of several meters is likely between the cores, 3G being deeper than 5G for the same

Comment #2   ing 3G of 3 m towards smaller depths roughly puts 3G and 5G in phase in this depth
       interval.

       This synchronisation during termination II adds one more tie point to the scheme of Vostok cores
260   synchronisation (see Figure 3), mainly based on tephra synchronisation [Basile, 1997].

2.2.4 EDC99/VK-5G and EDC99/VK-BH7 synchronisations

An initial prior synchronization between Vostok and EDC was previously done using the deuterium records [Parrenin et al., 2007b]. This synchronisation was later refined using the ECM record from the Vostok 5G and BH7 ice cores, the sulfate record from the EDC96 ice core and the ECM, DEP and sulfate records from the EDC99 ice core. The EDC96 sulfate and ECM data were transferred to EDC99 depths using the volcanic synchronisation between EDC96 and EDC99, while the BH7 depths were transferred to 5G using the volcanic synchronisation as previously explained.

Two different operators have conducted the volcanic synchronisation work (FP and EWW) and one other operator has checked specific time periods (MS). In total, 111 volcanic tie points were derived and are listed in Table 3 and Table 4.

During the process of volcanic synchronisation, we use the pattern of peaks with age rather than just the height of peaks. In this way we could consider if the distortions in layer thickness required to match Vostok to the EDC age scale are reasonable. For EDC, we used the EDC3 age scale [Parrenin et al., 2007b] while for Vostok our prior age scale is VK-FGT1 [Parrenin et al., 2004]. For this we used the ratio of the duration of one time interval in the Vostok and EDC glaciological time scales (see Figure 7). We tried to keep this ratio as close as possible to 1 and as smooth as possible.

The synchronisation is convincing for the period 105-145 kyr BP but is more difficult during glacial times and for the Holocene. This might be partly due to poor quality of the Vostok ECM record covering the brittle zone.

For the period 0-45 kyr BP, we revisited the synchronisation by Udisti et al. [2004] and we in particular removed several tie points which were judged as too uncertain. Our approach is thus more conservative than the approach by Udisti et al. [2004].

3 Discussion

3.1 *Climatic implications: EDC-VK isotope phasing*

In the following we investigate the phasing between EDC-(96,99) and VK-3G isotope records, taking into account the volcanic synchronisation which has been done using the VK-5G ice core. We now assume VK-3G depths can be directly transferred to VK-5G. Indeed, the VK-3G/VK-5G correspondences described in Figure 3 are too sparse to be used continuously. The resulting EDC-VK isotopic phasing – or time delay – is plotted in Figure 7. It has been computed as the difference between two EDC3-based Vostok chronologies, one based on volcanic synchronisation (this study) and one using the isotopic synchronisation [Parrenin et al., 2007b]. A positive value of this phasing means that the EDC isotopic record is younger with respect to the VK isotopic record. This phasing

roughly falls between -100 and 900 yr back to 100 kyr. It then reaches -1600 yr at 115 kyr BP and oscillates between -1000 and 0 yr between 120 and 145 kyr BP.

295   Unfortunately, the ECM data used for the volcanic synchronisation are measured on the VK-5G core while the deuterium data have been measured on the VK-3G core. The observed time delay between the EDC and Vostok isotope records can therefore arise either from real isotopic phasing differences or as a consequence of depth shifts between the VK-3G and VK-5G cores. However, at 100 kyr BP, 1 m of ice at Vostok typically represents 100 yr. It seems thus unlikely that the extreme

300   values of the time delay (typically 1-1.5 kyr) can be explained by depth shifts only: the shift would need to reach up to about 10-15 m in such case. Although difficult to explain, a significant isotopic phasing difference between the Vostok and EDC sites cannot be ruled out, in particular during the time interval 95-120 kyr BP, corresponding to the inception of the last glacial period.Indeed isotopic differences have been observed in various Greenlandic ice cores [Rasmussen et al., 2008], although

305   these differences ~~concerned the levels~~ and not the relative phasing. Moreover, significant differences between Vostok and EDC have been observed in the deuterium excess record during the inception of the last glaciation [Vimeux et al., 1999; Stenni et al., 2010]. But we would like first to better assess these isotopic differences, in particular in measuring the VK-5G δD profile on this time interval. This will be ~~treated~~ in a future study.

310   We thus highlight here the limits of the isotopic synchronisation, in particular when the isotopic records have different shapes [Sime et al., 2009; Masson-Delmotte et al., 2010]. Several processes can cause different isotopic trends: differences in moisture transport, precipitation intermittency bias, elevation, variable contribution from different moisture sources.

See comment #3

During termination II (see Figure 8), after synchronizing the EDC and Vostok ice cores, the two

315   isotope records indicate a significant phase lag (about 500 years, termination II apparently being recorded earlier in Vostok). The high resolution isotope measurements performed on the Vostok 5G core for the 125-135 kyr BP time interval (light green curve) does not exhibit this phase lag.

3.2 Glaciological implications

The Vostok – EDC depth to depth relationship (Figure 9) indicates a change to lower slope at

320   around 500 m Vostok-depth (corresponding to ~32 kyr on the EDC3 age scale) which persists throughout the ice ~~covering~~ the last interglacial period. This corresponds to thicker layers below 500 m depth than in younger ice for the Vostok record relative to EDC. The are two factors explaining these large annual layers at Vostok below 500 m depth. First, the thinning function increases between 400 m and 800 m at Vostok because of a higher bedrock upstream of the Vostok station

325   [Parrenin et al., 2004]. Second, along the flow line, the ice 500 m deep at Vostok originates ~37-39

km upstream [Parrenin et al., 2004; Salamatin et al., 2009], where the accumulation rate is 30% larger than for sites close to the station and over the Lake Vostok region, as recontructed from isochrone layers [Salamatin et al., 2009]. We should note however that measurements of recent snow accumulation upstream of Vostok do not reveal this upstream increase of accumulation [Eykakin, personnal communication]. Such an upstream increase may thus be only valid for the past. Indeed, the existing preliminary data on accumulation and isotopes in the surface snow in the area of Lake Vostok suggest [Ekaykin, personnal communication] that the Vostok Station and the Vostok flow line are currently located in the vicinity of the boundary between Indian and Pacific air masses, which makes accumulation (and the isotopic content of snow) in this region especially sensitive to possible changes in position of this boundary in the past.

Parrenin et al. [2004] took into account these two parameters (higher accumulation rate and bedrock elevation upstream of Vostok station) when producing the modelled VK-FGT1 time scale. We can now compare in details this time scale with the EDC3 time scale for the EDC ice core using the volcanic synchronisation (see Figure 10). We can note that the agreement is very good back to 100 kyr: the difference never exceeds ~1 kyr, which means that spatial variations of accumulation rate and bedrock elevation alone can explain the change of slope at ~500 m depth at Vostok. Our interpretation of the change of slope in the EDC-depth / VK-depth diagram, based on the spatial variation of accumulation upstream of Vostok, is different from the interpretation by Udisti et al., [2004] concentrating on the relative temporal variations of accumulation. We think that we have at this point no firm data to conclude that the temporal variations of accumulation were different at the two sites, even if this hypothesis cannot be completely dismissed.

Comment #4

The VK-FGT1 – EDC3 difference decreases below -3 kyr in the 105-110 kyr interval and increases again to ~3 kyr at 150 kyr BP. It means that the time interval 105-150 kyr BP is 6 kyr longer in VK-FGT1 than in EDC3. The reconciliation between these two glaciological dating models requires further investigations. It will be particularly useful to assess the accuracy of the assumptions in the relationships between stable isotopes and accumulation.

Comment #5

3.3 The ~73 kyr BP Toba eruptive event

Before searching for signs of the Toba in the Antarctic ice, it would be important to know if there were only one or several eruptive events during this time period, as has sometimes been claimed. Westgate et al. [1998] unequivocally demonstrated that all the presently known Toba tephra occurrences in peninsular India belong to the 73 kyr BP Toba super-eruption. There were however several known eruptions of this volcano during the Quaternary [see Westaway et al., 2011, for an exhaustive review].

Previous radiometric ages for the ~73 kyr BP Toba super-eruption range from an isothermal plateau,
fission track age of 68±7 kyr on glass from a deposit in Malaysia [Chesner et al., 1991] to K-Ar
ages of 75±12 and 74±3 kyr on tuff deposits [Ninkovitch et al., 1978] and an Ar-Ar age of 73±4 kyr
also on sanidine from the tuff [Chesner et al., 1991]. This leaves a large number of candidates in the
Antarctic ice: between 69 and 77 kyr BP, there are about 10 relatively large spikes in the EDC and
Vostok records (see Figure 11), none being exceptional in terms of amplitude.

To refine the search for the Toba volcanic signature, we account for the fact that Zielinski et al.
[1996] found a huge sulphate spike in GISP2 ice core which they attributed to the Toba mega
eruption at the end of GI-20. Following the classical seesaw hypothesis [Stocker and Johnsen,
2003], inspired by Blunier and Brook [2001] for this time period using the Byrd and GISP2 ice
cores, and refined using the NorthGRIP-EDML synchronisation [Capron et al., 2010], the end of a
Greenland Interstadial (GI) is contemporaneous with the onset of Southern ocean warming.
Assuming no phase lag between Southern Ocean warming and rising $\delta^{18}O/\delta D$ values in Antarctic
precipitation, the GI-20 in the GISP2 should thus correspond to the trough between Antarctic
Isotope Maximums (AIM) 19 and 20 in the Vostok and EPICA Dome C isotope records. During this
time period in both Antarctic records, ECM records display three large spikes that may represent the
corresponding counterpart of this event (see Figure 11). These spikes are also present in the EDC
DEP and sulphate records. However, they are not significantly larger than many other peaks in the
records.

4 Conclusion and outlook

111 volcanic tie points between EDC and Vostok are proposed in the 0-145 kyr BP time interval,
updating and complementing the previous 56 tie points reported for the time interval 0-45 kyr by
Udisti et al. [2004]. This new synchronisation will stand as a foundation for the establishment of the
next synchronized Antarctic ice core dating, as an updated EDC3. The synchronization is robust for
the last interglacial period (105-145 kyr) but is more difficult to constrain during the last glacial
period and the Holocene, in particular due to poor quality of the Vostok ECM record (e.g. brittle
zone). This synchronisation will be extended for older time periods and to other ice cores (Dome
Fuji, WAIS, etc.) in further studies. We suggest that significant isotopic phase differences could
exist between EDC and Vostok during the time interval 95-120 kyr BP but the lack of isotopic data
from the 5G ice core prevents a precise investigation of this phasing. At time of Termination II
where 5G isotope data exist, the EPICA Dome C and Vostok (5G) isotope (climate) records display
no significant phase lag. A change of slope in the VK-depth/EDC-depth diagram is explained by a
larger surface accumulation rate upstream of Vostok as well as less thinned layers in depth at
Vostok. Contrary to Udisti et al. [2004], we did not invoke any significant temporal relative change

of accumulation between the Vostok and EDC sites, even if this later hypothesis cannot be dismissed. For the period ~72.5 kyr BP, three major spikes on the volcanic records from the two

395 Antarctic ice cores may correspond to a huge sulphate spike found in Greenland GISP2 and attributed to the Toba eruption event. The search for glass shards for securely pinpointing the volcanic source is under consideration.

5 References

Barnes, P. R. F.; Wolff, E. W. & Mulvaney, R. (2006), 'A 44 kyr paleoroughness record of the Antarctic surface', *J. Geophys. Res.* **111**(D3), D03102.

Basile, I. (1997), 'Origine des aérosols volcaniques de la carotte de glace de Vostok (Antarctique)', PhD thesis, Univ. Joseph Fourier.

Blunier, T. & Brook, E. J. (2001), 'Timing of millennial-scale climate change in Antarctica and Greenland during the last glacial period', *Science* **291**(5501), 109-112.

Capron, E.; Landais, A.; Chappellaz, J.; Schilt, A.; Buiron, D.; Dahl-Jensen, D.; Johnsen, S. J.; Jouzel, J.; Lemieux-Dudon, B.; Loulergue, L.; Leuenberger, M.; Masson-Delmotte, V.; Meyer, H.; Oerter, H. & Stenni, B. (2010), 'Millennial and sub-millennial scale climatic variations recorded in polar ice cores over the last glacial period', *Climate of the Past* **6**(3), 345--365.

Castellano, E.; Becagli, S.; Hansson, M.; Hutterli, M.; Petit, J. R.; Rampino, M. R.; Severi, M.; Steffensen, J. P.; Traversi, R. & Udisti, R. (2005), 'Holocene volcanic history as recorded in the sulfate stratigraphy of the European Project for Ice Coring in Antarctica Dome C (EDC96) ice core', *J. Geophys. Res.* **116**, D06114.

Chesner, C. A.; Rose, W. I.; Deino, A.; Drake, R. & Westgate, J. A. (1991), 'Eruptive history of Earth's largest Quaternary caldera (Toba, Indonesia) clarified', *Geology* **19**, 200-203.

Dreyfus, G. B.; Parrenin, F.; Lemieux-Dudon, B.; Durand, G.; Masson-Delmotte, V.; Jouzel, J.; Barnola, J.-M.; Panno, L.; Spahni, R.; Tisserand, A.; Siegenthaler, U. & Leuenberger, M. (2007), 'Anomalous flow below 2700 m in the EPICA Dome C ice core detected using $\delta^{18}O$ of atmospheric oxygen measurements', *Climate of the Past* **3**(2), 341--353.

Ekaykin, A. A.; Lipenkov, V. Y.; Barkov, N. I.; Petit, J.-R. & Masson-Delmotte, V. (2002), 'Spatial and temporal variability in isotope composition of recent snow in the vicinity of Vostok station, Antarctica: implications for ice-core record interpretation', *Annals of Glaciology* **35**, 181-186.

EPICA community members (2004), '8 glacial cycles from an Antarctic ice core', *Nature* **429**, 623-628.

Frezzotti, M.; Pourchet, M.; Flora, O.; Gandolfi, S.; Gay, M.; Urbini, S.; Vincent, C.; Becagli, S.; Gragnani, R.; Proposito, M.; Severi, M.; Traversi, R.; Udisti, R. & Fily, M. (2005), 'Spatial and temporal variability of snow accumulation in East Antarctica from traverse data', *J. Glaciol.* **51**(172), 113-124.

Gao, C.; Robock, A. & Ammann, C. (2008), 'Volcanic forcing of climate over the past 1500 years: An improved ice core-based index for climate models', *J. Geophys. Res.* **113**(D23), D23111.

Gao, C.; Robock, A.; Self, S.; Witter, J. B.; Steffenson, J. P.; Clausen, H. B.; Siggaard-Andersen, M.-L.; Johnsen, S.; Mayewski, P. A. & Ammann, C. (2006), 'The 1452 or 1453 A.D. Kuwae eruption signal derived from multiple ice core records: Greatest volcanic sulfate event of the past 700 years', *J. Geophys. Res.* **111**, 1-11.

Goujon, C.; Barnola, J.-M. & Ritz, C. (2003), 'Modeling the densification of polar firn including heat diffusion: application to close-off characteristics and gas isotopic fractionation for Antarctica and Greenland sites', *J. Geophys. Res.* **108**(D24), ACL10/1-10.

455   Hagemann, R. & Lohez, P. (1978), 'Deuterium / hydrogen isotope ratio analysis', *Advances in Mass Spetrometry* **74**, 504-509.

Jouzel, J.; Lorius, C.; Petit, J.-R.; Genthon, C.; Barkov, N. I.; Kotlyakov, V. & Petrov, V. M. (1987), 'Vostok ice core: A continuous isotope temperature record over the last climatic cycle (160,000
460   years)', *Nature* **329**(6138), 403-408.

Jouzel, J.; Masson, V.; Cattani, O.; Falourd, S.; Stievenard, M.; Stenni, B.; Longinelli, A.; Johnsen, S.; Steffenssen, J.; Petit, J.; Schwander, J.; Souchez, R. & Barkov, N. I. (2001), 'A new 27 kyr high resolution East Antarctic climate record', *Geophys. Res. Let* **28**(16), 3199-3202.
465
Jouzel, J.; Masson-Delmotte, V.; Cattani, O.; Dreyfus, G.; Falourd, S.; Hoffmann, G.; Minster, B.; Nouet, J.; Barnola, J. M.; Chappellaz, J.; Fischer, H.; Gallet, J. C.; Johnsen, S.; Leuenberger, M.; Loulergue, L.; Luethi, D.; Oerter, H.; Parrenin, F.; Raisbeck, G.; Raynaud, D.; Schilt, A.; Schwander, J.; Selmo, E.; Souchez, R.; Spahni, R.; Stauffer, B.; Steffensen, J. P.; Stenni, B.;
470   Stocker, T. F.; Tison, J. L.; Werner, M. & Wolff, E. W. (2007), 'Orbital and Millennial Antarctic Climate Variability over the Past 800,000 Years', *Science* **317**(5839), 793-796.

Kawamura, K.; Parrenin, F.; Uemura, R.; Vimeux, F.; Severinghaus, J. P.; Matsumoto, K.; Nakata, H.; Nakazawa, T.; Aoki, S.; Jouzel, J.; Fujii, Y. & Watanabe, O. (2007), 'Northern Hemisphere
475   forcing of climatic cycles over the past 360,000 years implied by absolute dating of Antarctic ice cores', *Nature* **448**, 912-917.

Laepple, T.; Werner, M. & Lohmann, G. (2011), 'Synchronicity of Antarctic temperatures and local solar insolation on orbital timescales', *Nature* **471**(7336), 91--94.
480
Masson-Delmotte, V.; Buiron, D.; Ekaykin, A.; Frezzotti, M.; Gallée, H.; Jouzel, J.; Krinner, G.; Landais, A.; Motoyama, H.; Oerter, H.; Pol, K.; Pollard, D.; Ritz, C.; Schlosser, E.; Sime, L. C.; Sodemann, H.; Stenni, B.; Uemura, R. & Vimeux, F. (2011), 'A comparison of the present and last interglacial periods in six Antarctic ice cores', *Climate of the Past* **7**(2), 397--423.
485
Narcisi, B.; Petit, J.-R. & Tiepolo, M. (2006), 'A volcanic marker (92 ka) for dating deep east Antarctic ice cores', *Quat. Sci. Rev.* **25**, 2682-2687.

Ninkovich, D.; Shackleton, N. J.; Abdel-Monem, A. A.; Obradovich, J. D. & Izett, G. (1978), 'K-Ar
490   age of the Pleistocene eruption of Toba, north Sumatra', *Nature* **276**, 574-577.

Parrenin, F.; Barnola, J.-M.; Beer, J.; Blunier, T.; Castellano, E.; Chappellaz, J.; Dreyfus, G.; Fischer, H.; Fujita, S.; Jouzel, J.; Kawamura, K.; Lemieux-Dudon, B.; Loulergue, L.; Masson-Delmotte, V.; Narcisi, B.; Petit, J.-R.; Raisbeck, G.; Raynaud, D.; Ruth, U.; Schwander, J.; Severi,
495   M.; Spahni, R.; Steffensen, J. P.; Svensson, A.; Udisti, R.; Waelbroeck, C. & Wolff, E. (2007b), 'The EDC3 chronology for the EPICA Dome C ice core', *Clim. Past* **3**, 485-497.

Parrenin, F.; Dreyfus, G.; Durand, G.; Fujita, S.; Gagliardini, O.; Gillet, F.; Jouzel, J.; Kawamura, K.; Lhomme, N.; Masson-Delmotte, V.; Ritz, C.; Schwander, J.; Shoji, H.; Uemura, R.; Watanabe,
500   O. & Yoshida, N. (2007a), 'Ice flow modelling at EPICA Dome C and Dome Fuji, East Antarctica', *Clim. Past* **3**, 243-259.

Parrenin, F.; Rémy, F.; Ritz, C.; Siegert, M. & Jouzel, J. (2004), 'New modelling of the Vostok ice flow line and implication for the glaciological chronology of the Vostok ice core', *J. Geophys. Res.*
505   **109**, D20102.

Petit, J. R.; Jouzel, J.; Raynaud, D.; Barkov, N. I.; Barnola, J.-M.; Basile, I.; Bender, M.; Chappellaz, J.; Devis, M.; Delaygue, G.; Delmotte, M.; Kotlyakov, V. M.; Legrand, M.; Lipenkov, V. Y.; Lorius, C.; Pepin, L.; Ritz, C.; Saltzman, E. & Stievenard, M. (1999), 'Climate and atmospheric history of the past 420,000 years from the Vostok ice core, Antarctica', *Nature* **399**(6735), 429-436.

Petraglia, M.; Korisettar, R.; Boivin, N.; Clarkson, C.; Ditchfield, P.; Jones, S.; Koshy, J.; Lahr, M. M.; Oppenheimer, C.; Pyle, D.; Roberts, R.; Schwenninger, J.-L.; Arnold, L. & White, K. (2007), 'Middle Paleolithic Assemblages from the Indian Subcontinent Before and After the Toba Super-Eruption', *Science* **317**(5834), 114-116.

Raisbeck, G. M.; Yiou, F.; Jouzel, J. & Stocker, T. F. (2007), 'Direct north-south synchronization of abrupt climate change record in ice cores using Beryllium 10', *Clim. Past* **3**(3), 541—547.

Rasmussen, S.; Seierstad, I.; Andersen, K.; Bigler, M.; Dahl-Jensen, D. & Johnsen, S. (2008), 'Synchronization of the NGRIP, GRIP, and GISP2 ice cores across MIS 2 and palaeoclimatic implications', *Quaternary Science Reviews* **27**(1-2), 18 - 28.

Robock, A.; Ammann, C. M.; Oman, L.; Shindell, D.; Levis, S. & Stenchikov, G. (2009), 'Did the Toba volcanic eruption of ~74 ka B.P. produce widespread glaciation?', *J. Geophys. Res.* **114**(D10), D10107.

Salamatin, A. N.; Lipenkov, V. Y.; Barnola, J. M.; Hori, A.; Duval, P. & Hondoh, T. (2009), Snow-firn densification in polar ice sheets, *in* T. Hondoh, ed.,'Physics of Ice Core Records 2', Hokkaido University Press, Sapporo.

Salamatin, A. N.; Tsyganova, E. A.; Popov, S. V. & Lipenkov, V. Y. (2009), Ice flow line modeling in ice core data interpretation: Vostok Station (East Antarctica), *in* T. Hondoh, ed.,'Physics of Ice Core Records 2', Hokkaido University Press, Sapporo.

Severi, M.; Castellano, E.; Morganti, A.; Udisti, R.; Ruth, U.; Fischer, H.; Huybrechts, P.; Wolff, E.; Parrenin, F.; Kaufmann, P.; Lambert, F. & Steffensen, J. (2007), 'Synchronisation of the EDML1 and EDC3 timescales for the last 52 kyr by volcanic signature matching', *Clim. Past* **3**, 367-374.

Siddall, M.; Milne, G. A. & Masson-Delmotte, V. (2011), 'Uncertainties in elevation changes and their impact on Antarctic temperature records since the end of the last glacial period', *Earth and Planetary Science Letters* **In Press, Corrected Proof**, - .

Sime, L. C.; Wolff, E. W.; Oliver, K. I. C. & Tindall, J. C. (2009), 'Evidence for warmer interglacials in East Antarctic ice cores', *Nature* **462**(7271), 342--345.

Stenni, B.; Buiron, D.; Frezzotti, M.; Albani, S.; Barbante, C.; Bard, E.; Barnola, J. M.; Baroni, M.; Baumgartner, M.; Bonazza, M.; Capron, E.; Castellano, E.; Chappellaz, J.; Delmonte, B.; Falourd, S.; Genoni, L.; Iacumin, P.; Jouzel, J.; Kipfstuhl, S.; Landais, A.; Lemieux-Dudon, B.; Maggi, V.; Masson-Delmotte, V.; Mazzola, C.; Minster, B.; Montagnat, M.; Mulvaney, R.; Narcisi, B.; Oerter, H.; Parrenin, F.; Petit, J. R.; Ritz, C.; Scarchilli, C.; Schilt, A.; Schupbach, S.; Schwander, J.; Selmo, E.; Severi, M.; Stocker, T. F. & Udisti, R. (2011), 'Expression of the bipolar see-saw in Antarctic climate records during the last deglaciation', *Nature Geosci* **4**(1), 46--49.

Stenni, B.; Masson-Delmotte, V.; Selmo, E.; Oerter, H.; Meyer, H.; Röthlisberger, R.; Jouzel, J.; Cattani, O.; Falourd, S.; Fischer, H.; Hoffmann, G.; Iacumin, P.; Johnsen, S.; Minster, B. & Udisti,

R. (2010), 'The deuterium excess records of EPICA Dome C and Dronning Maud Land ice cores (East Antarctica)', *Quaternary Science Reviews* **29**(1-2), 146 - 159.

Stocker, T. F. & Johnsen, S. J. (2003), 'A minimum thermodynamic model for the bipolar seesaw', *Paleoceanography* **18**(4), 1-9.

Svensson, A.; Andersen, K. K.; Bigler, M.; Clausen, H. B.; Dahl-Jensen, D.; Davies, S. M.; Johnsen, S. J.; Muscheler, R.; Parrenin, F.; Rasmussen, S. O.; Röthlisberger, R.; Seierstad, I.; Steffensen, J. P. & Vinther, B. M. (2008), 'A 60 000 year Greenland stratigraphic ice core chronology', *Climate of the Past* **4**(1), 47--57.

Udisti, R.; Becagli, S.; Castellano, E.; Delmonte, B.; Jouzel, J.; Petit, J.-R.; Schwander, J.; Stenni, B. & Wolff, E. W. (2004), 'Stratigraphic correlations between the EPICA-Dome C and Vostok ice cores showing the relative variations of snow accumulation over the past 45 kyr', *J. Geophys. Res.* **109**(D8), D08101.

Udisti, R.; Becagli, S.; Castellano, E.; Mulvaney, R.; Schwander, J.; Torcini, S. & Wolff, E. W. (2000), 'Holocene electrical and chemical measurements from the EPICA-Dome C ice core', *Ann. Glaciol.* **30**, 20-26.

Vasiliev, N.; Talalay, P.; Bobin, N.; Chistyakov, V.; Zubkov, V.; Krasilev, A.; Dmitriev, A.; Yankilevich, S. & Lipenkov, V. (2007), 'Deep drilling at Vostok station, Antarctica: history and recent events', *Ann. Glaciol.* **47**(14), 10-23.

Vaughn, B.; White, J. W. C.; Delmotte, M.; Trolier, M.; Cattani, O. & Stievenard, M. (1998), 'An automated system for the uranium reduction method of hydrogen isotope analysis of water.', *Chemical Geology* **152**, 309-319.

Vimeux, F.; Masson, V.; Jouzel, J.; Stievenard, M. & Petit, J. R. (1999), 'Glacial-Interglacial changes in ocean surface conditions in the Southern Hemisphere', *Nature* **398**, 410-413.

Vinther, B. M.; Clausen, H. B.; Johnsen, S. J.; Rasmussen, S. O.; Andersen, K. K.; Buchardt, S. L.; Dahl-Jensen, D.; Seierstad, I. K.; Siggaard-Andersen, M.-L.; Steffensen, J. P.; Svensson, A.; Olsen, J. & Heinemeier, J. (2006), 'A synchronized dating of three Greenland ice cores throughout the Holocene', *J. Geophys. Res.* **111**, 13102.

Waelbroeck, C.; Franck, N.; Jouzel, J.; Parrenin, F.; Masson-Delmotte, V. & Genty, D. (2008), 'Transferring absolute dating of the Last Interglacial sea level high stand to marine and ice core records', *Earth Planet. Sci. Lett.* **265**, 183-194.

Waelbroeck, C.; Jouzel, J.; Labeyrie, L.; Lorius, C.; Labracherie, M. & Stiévenard, M. (1995), 'A comparison of the Vostok ice deuterium record and series from Southern Ocean core MD 88-770 over the last two glacial-interglacial cycles', *Clim. Dyn.* **12**(2), 113-123.

Watanabe, O.; Jouzel, J.; Johnsen, S.; Parrenin, F.; Shoji, H. & Yoshida, N. (2003), 'Homogeneous climate variability across East Antarctica over the past three glacial cycles', *Nature* **422**, 509-512.

Westaway, R.; Mishra, S.; Deo, S. & Bridgland, D. (2011), 'Methods for determination of the age of Pleistocene tephra, derived from eruption of Toba, in central India', *Journal of Earth System Science*, 1-28.

Westgate, J. A.; Shane, P. A. R.; Pearce, N. J. G.; Perkins, W. T.; Korisettar, R.; Chesner, C. A.;

610   Williams, M. A. J. & Acharyya, S. K. (1998), 'All Toba Tephra Occurrences across Peninsular India Belong to the 75,000 yr B.P. Eruption', *Quaternary Research* **50**(1), 107 - 112.

Williams, M. (2011, in press), 'Did the 73 ka Toba super-eruption have an enduring effect? Insights from genetics, prehistoric archaeology, pollen analysis, stable isotope geochemistry,
615   geomorphology, ice cores, and climate models', *Quat. Int..*

Williams, M. A.; Ambrose, S. H.; van der Kaars, S.; Ruehlemann, C.; Chattopadhyaya, U.; Pal, J. & Chauhan, P. R. (2009), 'Environmental impact of the 73 ka Toba super-eruption in South Asia', *Palaeogeography, Palaeoclimatology, Palaeoecology* **284**(3-4), 295 - 314.
620
Wolff, E.; Cook, E.; Barnes, P. & Mulvaney, R. (2005), 'Signal variability in replicate ice cores', *J. Glaciol.* **51**(174), 462-468.

Wolff, E. W. (2000), Electrical stratigraphy of polar ice cores: principles, methods, and findings, *in*
625   T. Hondoh, ed.,'Physics of Ice Core Records', Hokkaido University Press, Sapporo, pp. 462-468.

Wolff, E. W.; Basile, I.; Petit, J. R. & Schwander, J. (1999), 'Comparison of Holocene electrical records from Dome C and Vostok', *Ann. Glaciol.* **29**, 89-93.

630   Zielinski, G. A.; Mayewski, P. A. & Taylor, K. (1996), 'Potential atmospheric impact of the Toba mega-eruption 71,000 years ago', *Geophys. Res. Lett.* **23**(8), 837.

635

EDC96 depth (m)	EDC99 depth (m)
12,31	12,13
29.73	29.60
38.11	37.93
39.24	39.07
40.78	40.56
41.50	41.22
49.88	49.72
60.35	60.21
97.14	96.86
100.01	99.76
119.79	119.51
125.27	125.03
130.79	130.55
133.81	133.58
135.59	135.38
140.29	140.04
141.57	141.31
144.97	144.70
155.25	154.98
160.17	159.98
163.19	163.00
169.43	169.28
176.13	175.90
186.12	185.84
190.30	190.10
208.73	208.56
209.89	209.72
214.07	213.84
215.98	215.79
232.75	232.57
234.47	234.29
238.98	238.80
243.34	243.14
249.31	249.12
251.43	251.25
259.47	259.34
263.19	263.01
264.15	264.02

270.57	270.40
277.13	277.00
283.21	283.06
302.52	302.38
304.41	304.30
305.67	305.55
308.69	308.50
311.10	310.96
312.93	312.77
317.50	317.32
322.06	321.96
325.32	325.18
338.67	338.55
342.82	342.69
343.73	343.60
344.55	344.45
353.03	352.84
387.41	387.28
389.47	389.34
393.14	392.99
398.02	397.80
400.33	400.28
404.28	404.12
428.03	427.85
428.32	428.17
429.35	429.15
432.21	431.96
438.28	438.07
451.73	451.52
454.22	454.00
471.17	470.95
471.49	471.28
472.27	472.06
481.75	481.50
494.87	494.66
517.81	517.58
564.63	564.40
576.39	576.10
579.21	578.94

587.83	587.57
593.71	593.48
595.13	594.98
626.93	626.54
632.73	632.26
636.82	636.42
645.66	645.23
662.31	661.85
677.69	677.17
691.69	691.14
693.29	692.82
699.29	698.68
699.59	699.04
701.12	700.63
701.77	701.28
703.11	702.58
704.73	704.16
710.57	710.00
724.45	723.85
726.91	726.32
738.23	737.50
739.81	739.14
751.05	750.37
762.93	762.24
765.55	764.96
775.73	775.04
778.33	777.64

Table 1: List of volcanic tie points between the EDC96 and EDC99 ice cores using the DEP records.

VK-BH7 depth (m)	VK-5G depth (m)
102.12	104.68
212.76	216.01
218.38	221.77
220.35	223.70
225.20	228.59
233.33	236.76
233.95	237.30

Table 2: List of volcanic tie points between the VK-BH7 and VK-5G ice cores using the ECM records.

VK-BH7 depth (m)	VK-5G depth (m)
102.12	104.68
212.76	216.01
218.38	221.77
220.35	223.70
225.20	228.59
233.33	236.76
233.95	237.30

VK-BH7 depth (m)	Equiv. VK-5G depth (m)	EDC99 depth (m)
9.77	10.01	12.59
22.99	23.57	29.60
29.47	30.21	37.93
75.08	76.96	96.86
129.86	132.59	162.74
142.37	145.18	179.77
176.65	179.67	232.57
184.24	187.31	243.13

Table 3: List of volcanic tie points between the Vostok BH7 and EDC99 ice cores. The equivalent Vostok 5G depths are given for convenience, following the BH7-5G synchronisation discussed in the text.

VK-5G depth (m)	EDC99 depth (m)
289.94	387.31
291.41	389.32
294.21	393.00
302.92	404.14
328.62	438.09
372.65	492.53
374.29	494.64
422.85	553.12
432.36	564.39
496.49	632.23
511.15	645.92
547.33	677.14
642,28	777,65
644,94	780,58
652.77	787.15
657.45	790.52
658.85	791.87
665.45	798.49
766.44	874.22
821.24	914.44
879.35	961.22
947.52	1013.73
955.56	1019.45
983.80	1040.50
1023.50	1071.20
1035.00	1078.95
1036.00	1079.70
1038.45	1081.28
1043.56	1084.73
1048.35	1087.94
1063.00	1097.96
1063.96	1098.63
1119.53	1140.58
1156.55	1173.05
1160.50	1176.13
1164.35	1179.00
1206.42	1206.59
1244.91	1238.72
1283.45	1271.20
1291.80	1278.60
1332.60	1312.40
1334.65	1314.15
1337.60	1316.30
1372.44	1342.72

1374.64	1344.23
1386.73	1353.24
1465.02	1429.12
1478.49	1439.88
1483.12	1443.42
1488.81	1447.72
1489.70	1448.39
1493.34	1451.03
1495.23	1452.38
1498.50	1454.69
1500.34	1455.98
1501.33	1456.59
1521.75	1470.51
1537.39	1480.96
1540.20	1482.80
1550.39	1489.18
1559.18	1494.90
1571.15	1502.62
1576.67	1506.28
1582.09	1510.12
1584.00	1511.51
1618.24	1538.62
1621.23	1541.13
1637.66	1554.63
1648.56	1563.00
1662.08	1572.65
1673.03	1580.30
1673.74	1580.78
1674.22	1581.11
1682.91	1587.15
1699.71	1598.85
1707.25	1604.10
1711.50	1607.20
1715.55	1610.10
1743.59	1631.16
1801.70	1676.00
1805.43	1678.90
1811.99	1683.97
1820.80	1690.85
1828.30	1696.67
1838.34	1704.30
1844.60	1708.90
1847.65	1711.10
1855.50	1716.85

1869.70	1726.85
1876.63	1731.78
1880.80	1734.65
1896.85	1745.91
1899.85	1748.07
1926.70	1767.40
1929.00	1769.00
1932.75	1771.48
1934.90	1772.90
1948.70	1781.60
1950.95	1782.85
1962.65	1789.22
1966.36	1791.25
1982.00	1799.25
1991.93	1804.00

Table 4: List of volcanic tie points between the EPICA Dome C EDC99 and Vostok 5G ice cores.

Firetracc
(1998)

EDC96
(1996)

EDC99
(1999)

120

787.60

3259.72
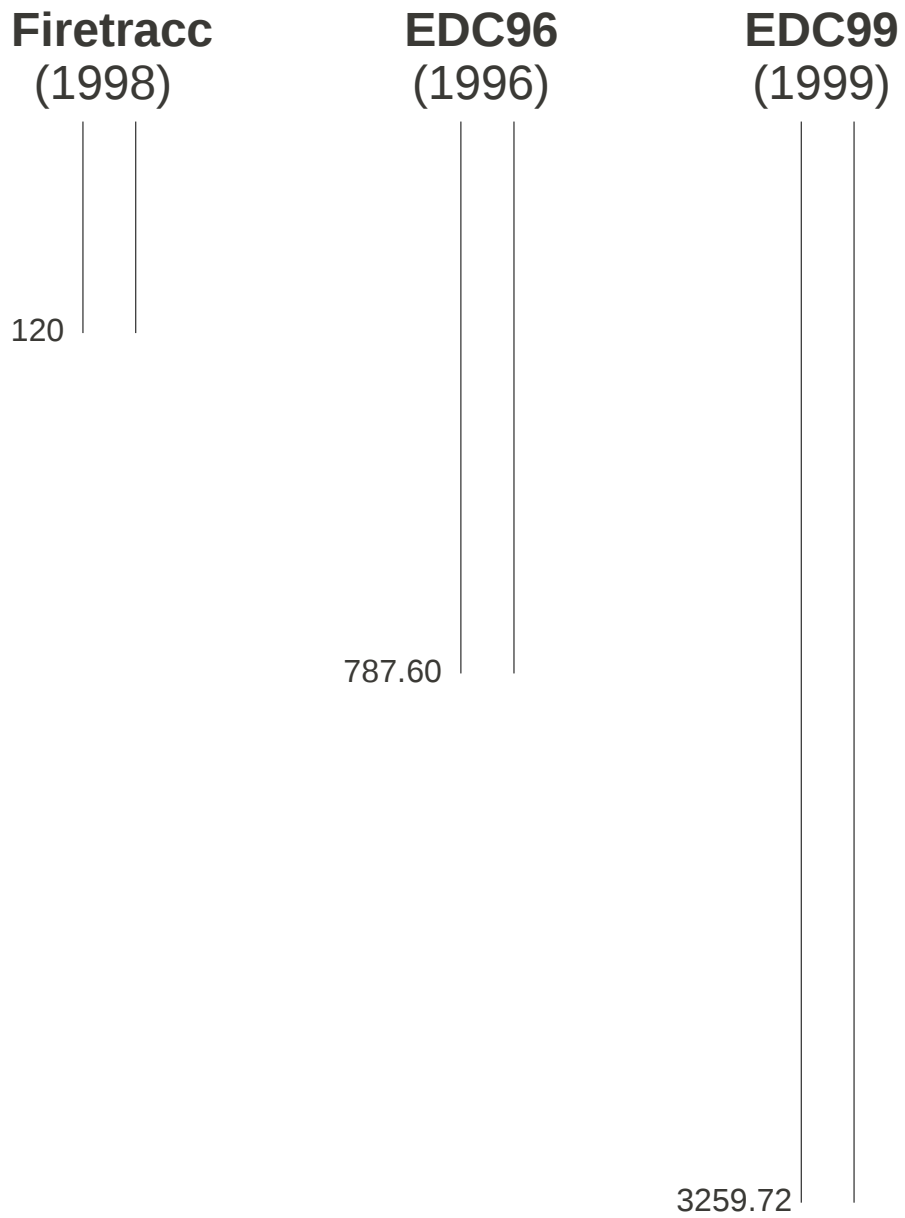
Figure 1: Scheme of the different EDC ice cores. The depths indicated are the maximum logging depths.

655
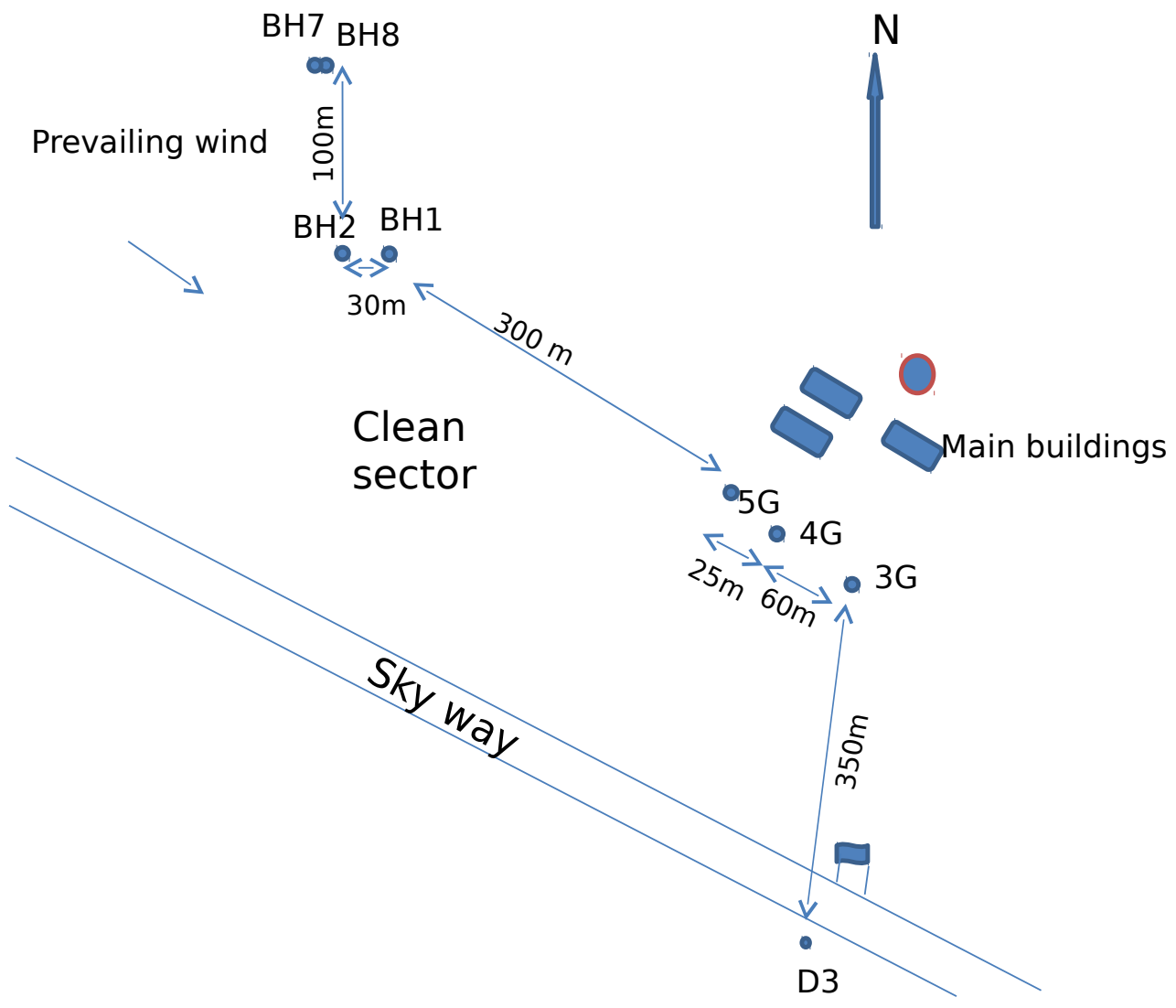
Figure 2: Map illustrating the location of the camp facilities as well as the different boreholes considered in this study at Vostok station.
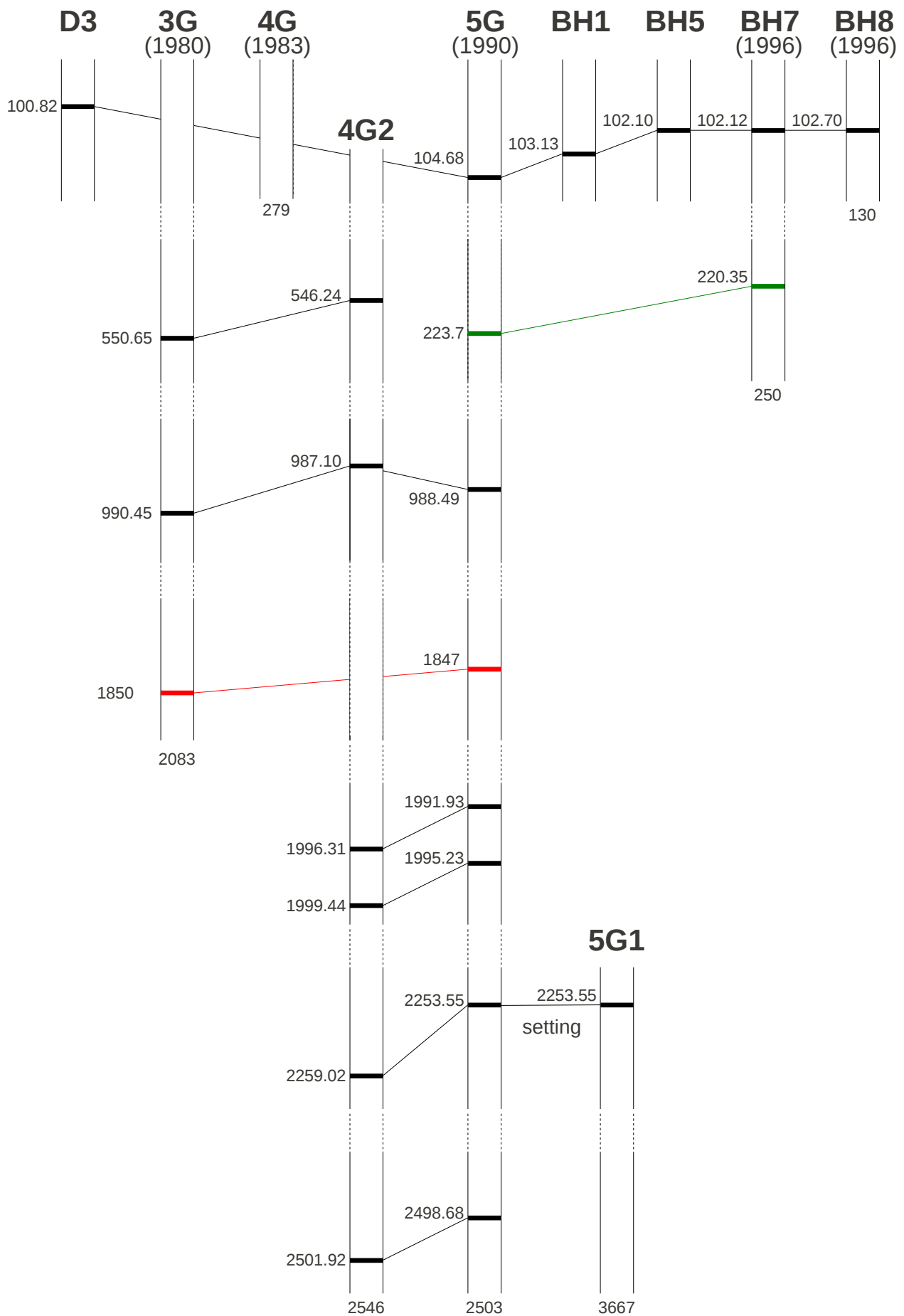
Figure 3: Scheme of the different Vostok cores and shifts between them based on tephra recognition (black), ice isotopes synchronisation (red) and ECM synchronisation (green).

A)
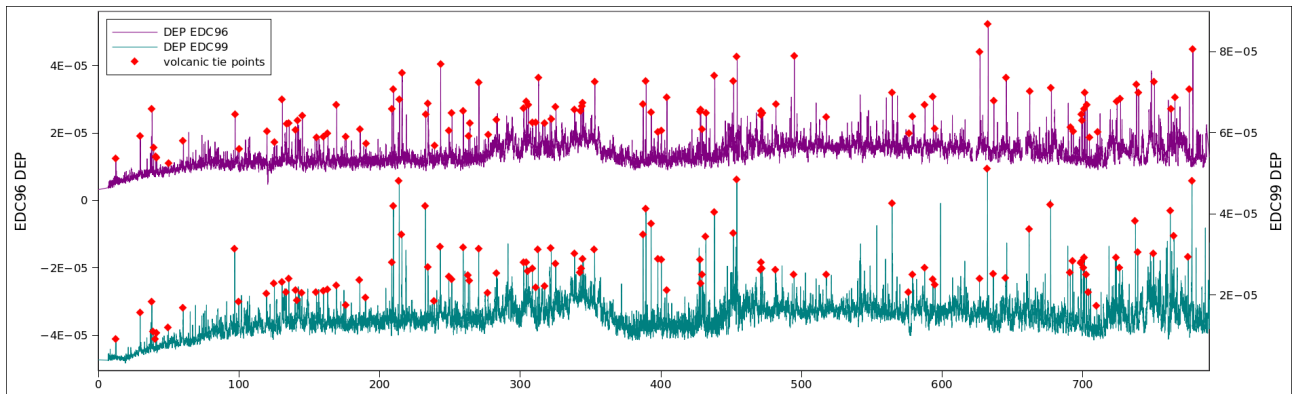
B)
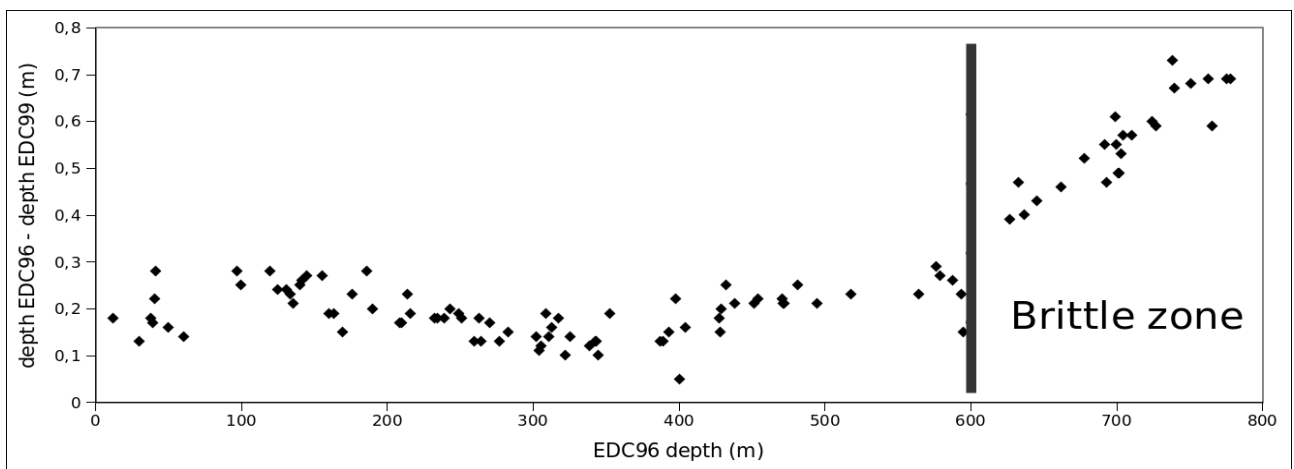
Figure 4: Volcanic synchronisation of the EDC96 and EDC99 ice cores using the DEP records.

A) DEP records and volcanic tie points.

B) Resulting depth offset between EDC96 and EDC99. The vertical bar marks the start of the brittle zone.

660
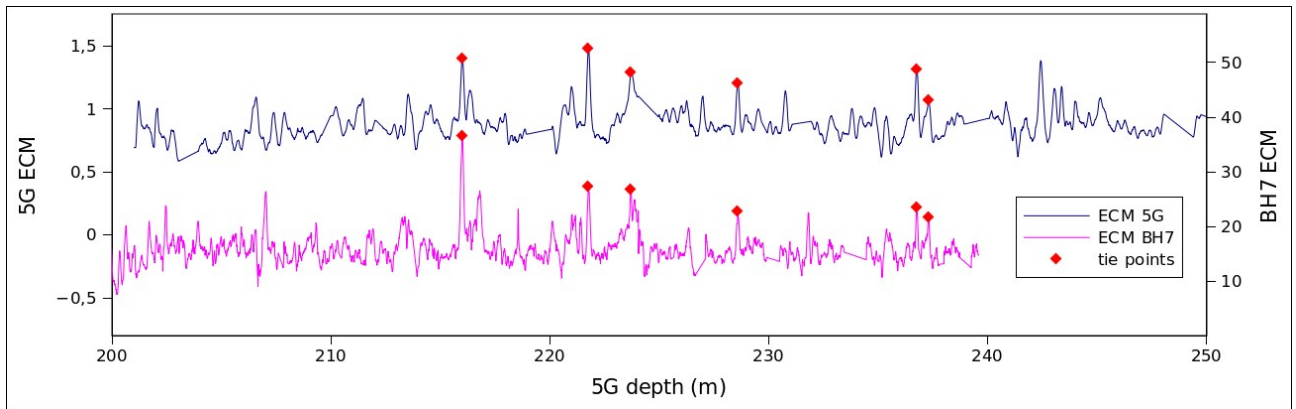
Figure 5: Volcanic synchronisation of the VK-BH7 and VK-5G ice cores using the ECM records.
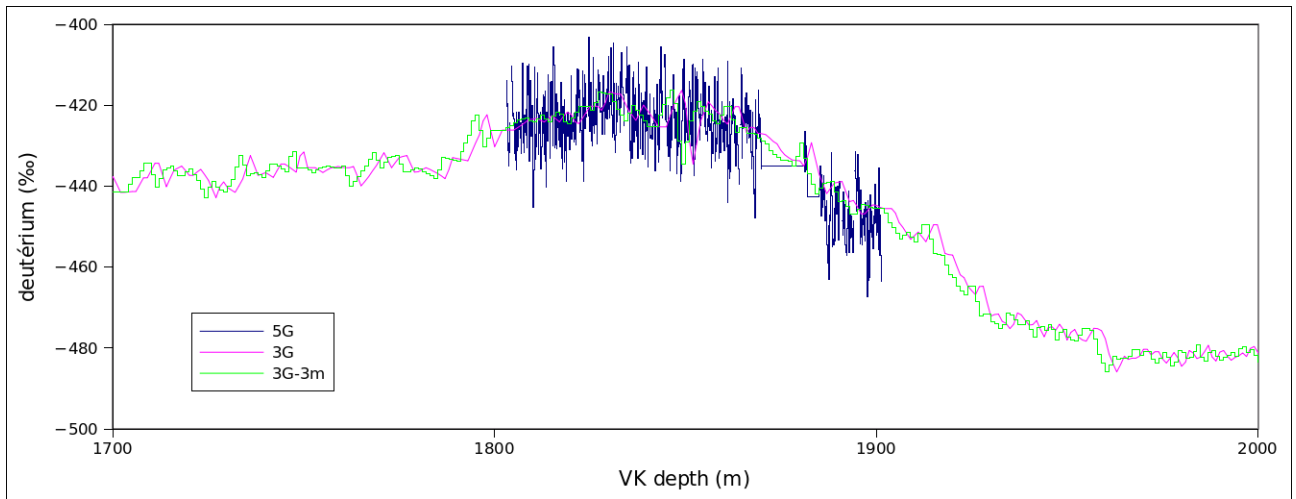
Figure 6: Vostok ice isotopic composition during termination II, for the 3G and 5G ice cores. A depth shift of several meters (typically 3 m) between both cores is likely.
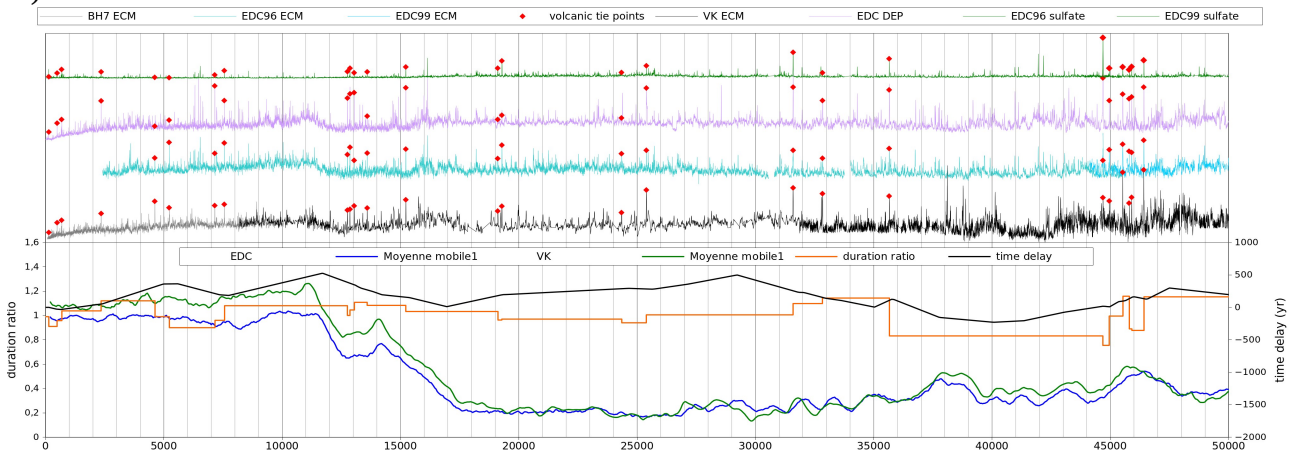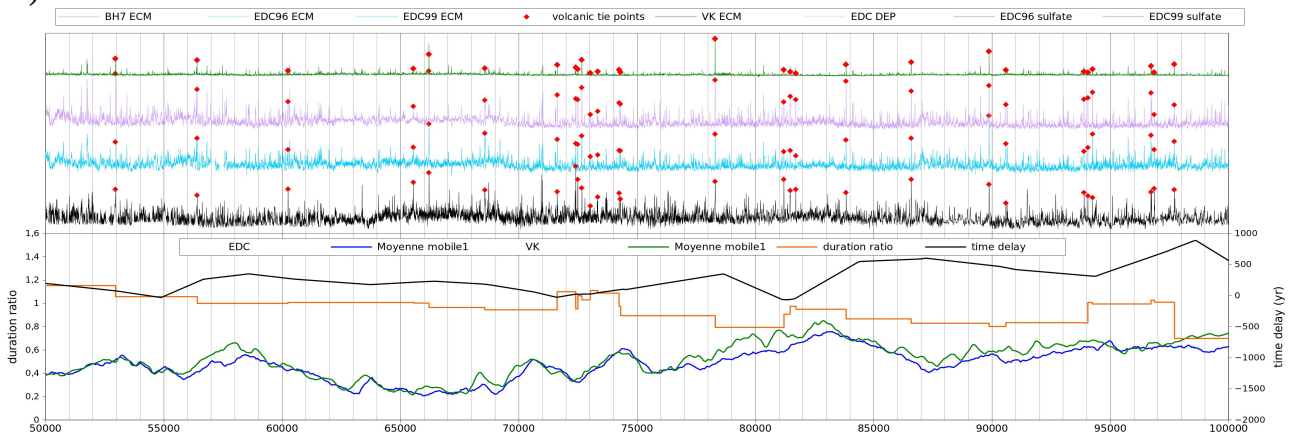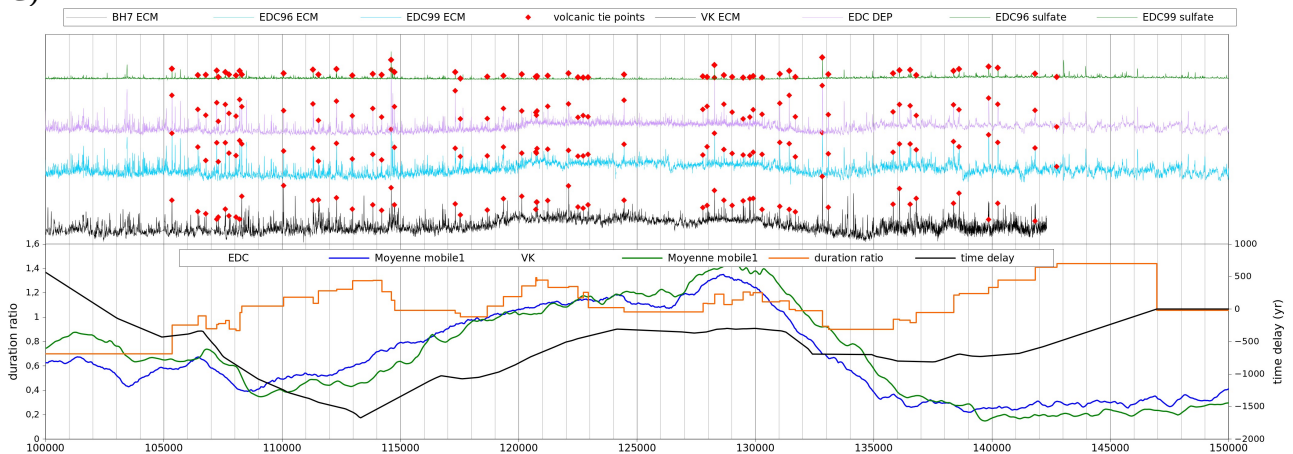
Figure 7: EDC/VK volcanic synchronisation on the EDC3 age scale.
A) 0-50 kyr BP; B) 50-100 kyr BP; C) 100-150 kyr BP
For A), B), C):
Top) Black: ECM record from the VK-5G ice core. Grey: ECM record from the VK-BH7 ice core.
Blue: ECM record from the EDC99 ice core. Pink: DEP record from the EDC99 ice core. Green:
sulfate records from the EDC96 and EDC99 ice cores. Red diamonds: volcanic tie points.
Bottom) Blue: Deuterium record from the EDC ice core. Green: Deuterium record from the Vostok
ice core. The deuterium records have been resampled every 50 yr and an 11 points moving average
was applied. Orange: ratio of the duration between two tie points in VK-FGT1 [Parrenin et al.,
2004] and EDC3 [Parrenin et al., 2007b]. Black: time delay between the VK-3G and EDC
deuterium records after volcanic synchronisation.
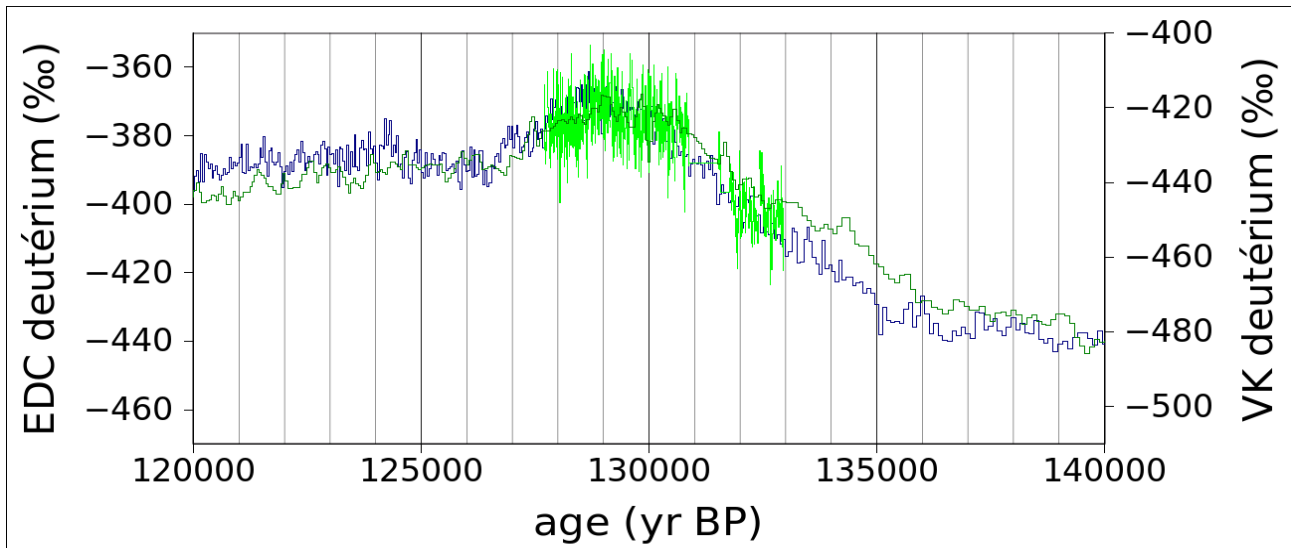
Figure 8: EDC/VK isotopic phasing during termination II after volcanic synchronisation

Blue: EDC deuterium record on its EDC3 age scale. Green: Vostok 3G deuterium record on the EDC3 age scale (after synchronisation, assuming 3G depths and 5G depths are synchronous). Light Green: Vostok 5G deuterium record on the EDC3 age scale (after synchronisation).
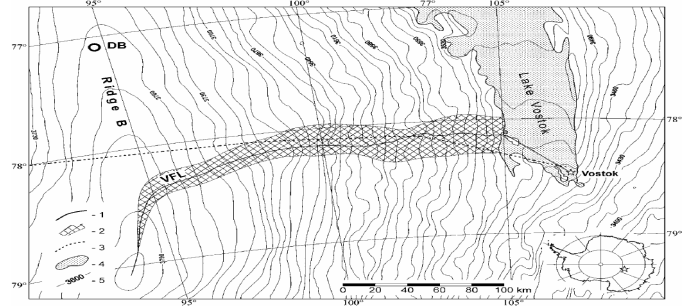
A)
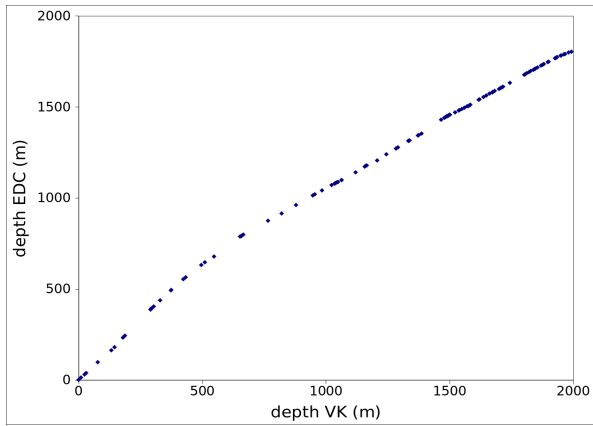
B)

Figure 9:

A) Volcanic tie points in a depth-VK / depth-EDC diagram.

B) The flow line between Ridge B and Vostok. Adapted from Salamatin et al. [2009].

The steep slope in graph A) between 0 and 500 m in VK corresponds to the lake part of the flow line, where the accumulation and berock elevation are lower than upstream.
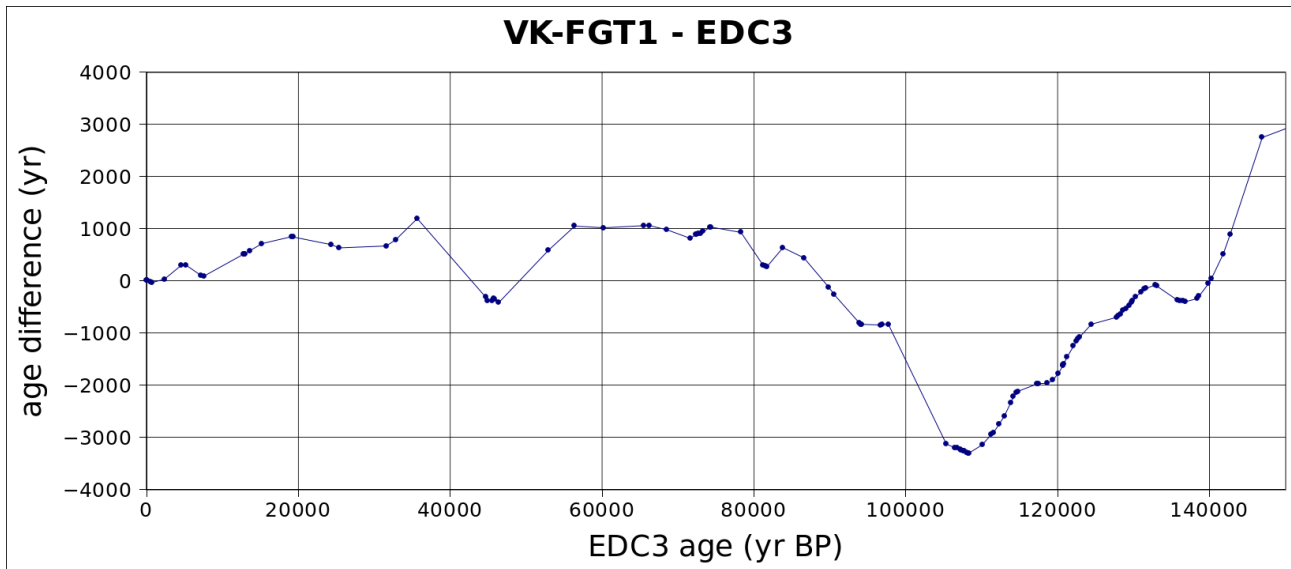
670

Figure 10: Comparison of the VK-FGT1 and EDC3 time scales at the volcanic synchronisation tie points.
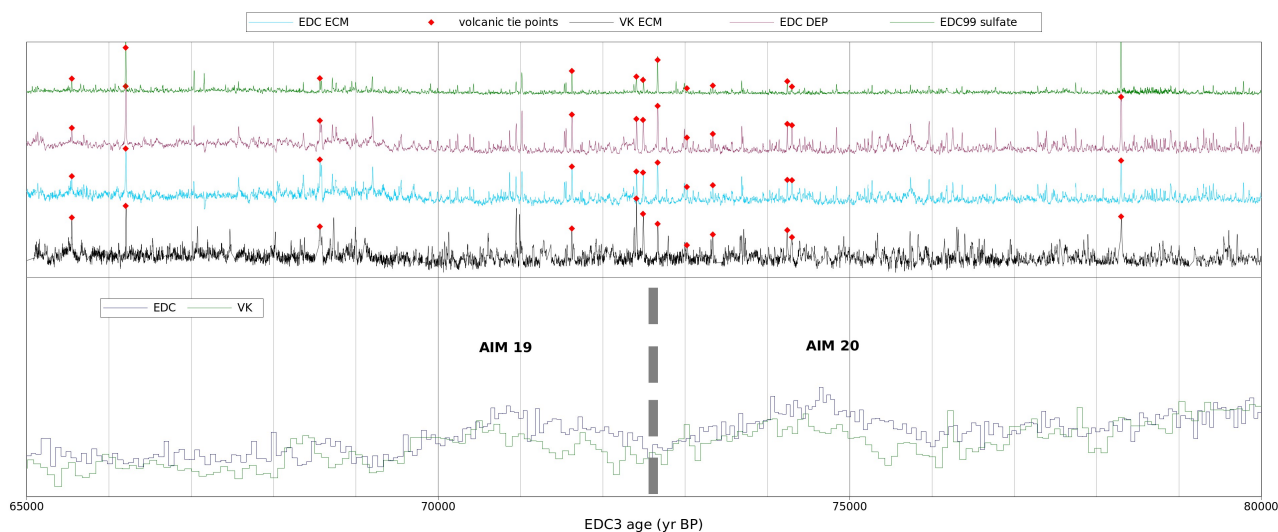
Figure 11: Synchronisation during the period 65-80 kyr BP including the Toba eruptive event on the EDC3 age scale.

Top) Black: ECM record from the VK-5G ice core. Blue: ECM record from the EDC99 ice core. Pink: DEP record from the EDC99 ice core. Green: sulfate records from the EDC96 and EDC99 ice cores. Red diamonds: volcanic tie points.

Bottom) Blue: Deuterium record from the EDC ice core. Green: Deuterium record from the Vostok ice core.